

# PET attenuation correction for PET/MR by combining MR segmentation and selective-update joint estimation

Lishui Cheng<sup>1</sup>, Sangtae Ahn<sup>1</sup>, Dattesh Shanbhag<sup>2</sup>, Florian Wiesinger<sup>3</sup>, Sandeep Kaushik<sup>2</sup>, and Ravindra Manjeshwar<sup>1</sup>

<sup>1</sup>GE Global Research, Niskayuna, NY, United States, <sup>2</sup>GE Global Research, Bangalore, India, <sup>3</sup>GE Global Research, Munich, Germany

## Purpose

PET/MR is an emerging hybrid imaging modality with promising opportunities in neurology, oncology and cardiology<sup>1</sup>. Despite significant technological advancements, accurate attenuation correction, critical to quantitative PET, still remains challenging. Segmentation of 3D gradient-echo (GRE) images is widely used in current MR-based attenuation correction (MR-AC) methods<sup>2-4</sup>. This enables reliable segmentation of soft tissue, including fat-water separation using Dixon-based methods<sup>5</sup>, for most of the imaging field-of-view (FOV) but it does not allow reliable decomposition of noisy MR regions into air, lung, bone and implants. On the other hand, PET attenuation and activity can be jointly estimated from PET emission data<sup>6,7</sup>. Although the inverse problem of joint estimation (JE) is highly ill-conditioned, PET time-of-flight (TOF) information<sup>8,9</sup> and prior anatomical knowledge<sup>10</sup> can significantly improve the conditioning and accuracy. In this work, we investigate a synergistic combination<sup>10</sup> of these two methods, starting with 1) segmentation-based MR-AC for regions of high confidence (i.e., soft-tissue and background air), followed by 2) resolving remaining uncertain MR regions (potentially containing internal air, lung, bone and implants) via selective-update JE, and evaluate on clinical data from a simultaneous PET/MR scanner with TOF PET.

## Methods

Whole-body, oncology patients were scanned on an investigational hybrid PET/MR scanner with TOF capability (GE Healthcare, Waukesha, WI, USA). A dedicated 3D GRE scan (FA=12°, FOV=50x50x33.3cm<sup>3</sup>, matrix=256x128x64, scan time=18s) with Dixon-type fat-water separation was acquired, followed by a body mask segmentation as described by Wollenweber *et al.*<sup>4</sup> From the MR histogram distribution, a threshold was derived, based on two level Huang threshold method, to differentiate between reliable soft-tissue signals and remaining uncertain regions within the body mask (potentially containing air, lung, bone and implants). The “MR-dark” region mask was consequently refined by using the lung and air mask obtained as described by Wollenweber *et al.*<sup>4</sup>. Then the soft-tissue region was assigned PET attenuation coefficient values corresponding to MR-derived fat-water fractions. Hardware attenuation information (i.e., table and rigid RF coils) was pasted from pre-acquired templates. Subsequently, TOF PET data were reconstructed using a selective-update JE approach<sup>10</sup> with attenuation information provided by the MR-segmentation based attenuation map only for high confidence regions (i.e., background air and soft-tissue). In the remaining uncertain regions, the attenuation was estimated jointly with the PET activity distribution. The attenuation in the uncertain regions and the activity were alternatively updated iteratively; the attenuation was updated by ordered subset transmission (OSTR) algorithm<sup>11</sup> with the attenuation in the high confidence regions as constraints, and the activity image was update by TOF ordered subset expectation maximization (OSEM)<sup>12</sup>. The quadratic penalty was used to encourage smoothness in the attenuation map. This method takes advantage of TOF information (timing resolution: ~400ps) provided by the scanner.

## Results

Figure 1 shows a demonstration of the method for a patient with spinal implants acquired on the hybrid PET/MR scanner. From left to right the figure displays the following data in transaxial and coronal views: (a) in-phase MR image used for segmenting MR-dark uncertain regions, which contain abdominal air and spinal bone/implant regions in this case, (b) MR-based attenuation map obtained as described in Wollenweber *et al.*<sup>4</sup> without using any prior anatomical knowledge, (c) MR-based attenuation map refined using prior anatomical knowledge (see Shanbhag *et al.*<sup>13</sup> for details), (d) attenuation map with the uncertain regions resolved via selective-update JE, and (e)-(g) PET images reconstructed by TOF OSEM with the attenuation maps (a)-(c), respectively. Using selective-update JE the uncertain regions were correctly resolved as abdominal internal air and spinal bone/implant regions (Fig. 1(d)), otherwise hidden in MR (Fig. 1(a)), translating in improved image quality of the corresponding PET images.

## Discussion/Conclusion

Standard segmentation-based MR-AC methods assign correct attenuation values for most of the 3D imaging FOV but fundamentally cannot resolve MR signal regions inside the body originating from air, lung, bone or implants. We presented a novel method which addresses this deficiency by 1) segmenting uncertain regions via low MR signal thresholding (plus morphologic refinements) and 2) using selective-update joint estimation to find attenuation values for these limited uncertain regions, which are most consistent with the measured PET data. The method demonstrated promising performance and was able to resolve uncertain low MR signal regions into abdominal air and bone/implant regions as well as lungs (Fig. 1). The selective-update JE approach takes advantage of 1) reliable attenuation information (e.g., soft-tissue) surrounding the uncertain regions obtained from MR and 2) excellent TOF characteristics of the PET/MR scanner used in this study. We also observed that use of a proton density weighted MR-AC protocol with uniform soft-tissue response and less T1 saturation of long T1 structures (i.e., muscle, CSF, blood, bladder and so on) is more favorable for uncertain segmentation.

## References

- [1] D. A. Torigian *et al.*, *Radiology* **267**, 26-44 (2013).
- [2] A. Martinez-Moller *et al.*, *J. Nucl. Med.* **50**, 520-526 (2009).
- [3] V. Schulz *et al.*, *Eur. J. Nucl. Med. Mol. Imaging* **38**, 138-152 (2011).
- [4] S. D. Wollenweber *et al.*, *IEEE Trans. Nucl. Sci.* **60**, 3391-3398 (2013).
- [5] W. T. Dixon, *Radiology* **153**, 189-194 (1984).
- [6] Y. Censor *et al.*, *IEEE Trans. Nucl. Sci.* **26**, 2775-2779 (1979).
- [7] J. Nuyts *et al.*, *IEEE Trans. Med. Imaging* **18**, 393-403 (1999).
- [8] M. Defrise *et al.*, *Phys. Med. Biol.* **57**, 885-899 (2012).
- [9] A. Rezaei *et al.*, *IEEE Trans. Med. Imaging* **31**, 2224-2233 (2012).
- [10] S. Ahn *et al.*, *Soc. Nucl. Med. Mol. Imaging (SNMMI) Annu. Meet. Abstr.* **54**, 150 (2013).
- [11] H. Erdogan & J. A. Fessler, *Phys. Med. Biol.*, **44**, 2835-2851 (1999).
- [12] H. M. Hudson & R. S. Larkin, *IEEE Trans. Med. Imaging* **13**, 601-609 (1994).
- [13] Shanbhag *et al.*, ISMRM (submitted) (2015).

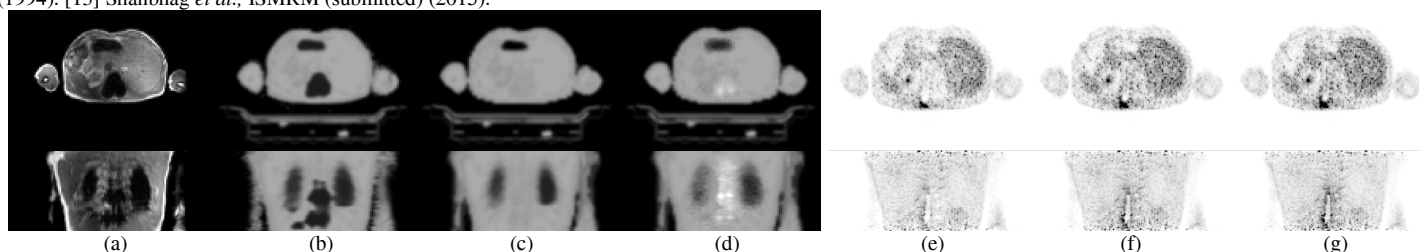


Figure 1: (a) In-phase MR image, (b) MR segmentation based attenuation map without any anatomical prior knowledge, (c) MR segmentation based attenuation map with anatomical prior knowledge, (d) attenuation map with uncertain regions resolved by selective-update joint estimation; and (e-g) PET images reconstructed by TOF OSEM using the attenuation maps in (b-d), respectively.